JACC: CARDIOVASCULAR INTERVENTIONS VOL. 3, NO. 8, 2010

ISSN 1936-8798/$36.00
PUBLISHED BY ELSEVIER INC. DOI: 10.1016/j.jcin.2010.05.011

3-Dimensional Optical Coherence Tomography Assessment of Jailed Side Branches by Bioresorbable Vascular Scaffolds

A Proposal for Classification

Takayuki Okamura, MD, PhD,* Yoshinobu Onuma, MD,*
Héctor M. García-García, MD, PhD,* Evelyn Regar, MD, PhD,*
Joanna J. Wykrzykowska, MD,* Jacques Koolen, MD,† Leif Thuesen, MD,‡
Stefan Windecker, MD,§ Robert Whitbourn, MD,‖ Dougal R. McClean, MD,¶
John A. Ormiston, MD,# Patrick W. Serruys, MD, PhD,*
on behalf of the ABSORB Cohort B Investigators

Rotterdam and Eindhoven, the Netherlands; Aarhus, Denmark; Bern, Switzerland; Fitzroy, Australia; and Christchurch and Auckland, New Zealand

Objectives The purpose of this study is to assess jailing of side branches (SB) by the everolimus-eluting, bioresorbable vascular scaffold (BVS) with 3-dimensional (3D) optical coherence tomography (OCT) reconstruction.

Background Because BVS struts at the SB orifice are suspected of being bioresorbed and/or forming a neointimal bridge, OCT has been used to evaluate the struts in detail at that particular site. Our understanding of the 3D relationship of the strut and the SB orifice is limited by the use of 2-dimensional OCT images. Fourier-domain OCT enables reliable 3D reconstruction of coronary vessels.

Methods The ABSORB Cohort B (A Clinical Evaluation of the Bioabsorbable Everolimus Eluting Coronary Stent System in the Treatment of Patients With de Novo Native Coronary Artery Lesions) trial is a multicenter single-arm trial to assess the safety and performance of the BVS. Fourier-domain OCT pullbacks (C7-XR system, LightLab Imaging Inc., Westford, Massachusetts) are obtained at pullback speed of 20 mm/s and 3D renderings are performed. The orifices of the SB are assessed visually. The area of SB orifice and the number of strut-free compartments delineated by the BVS struts are evaluated.

Results Fifty-one OCT pullbacks were acquired: 33 pullbacks were imaged with Fourier-domain OCT and 27 treated segments had 46 side branches. Three-dimensional assessment was feasible in 87% (40 of 46) of pullbacks. The mean area of the SB orifice was 1.16 ± 1.02 mm^2. The mean number of strut-free compartments was 2.0 ± 1.1. The classification of the overhanging struts is proposed.

Conclusions This study demonstrates that 3D OCT reconstruction is feasible to evaluate the orifices of SB jailed with BVS. (ABSORB Clinical Investigation, Cohort B; NCT00856856) (J Am Coll Cardiol Intv 2010;3:836–44) © 2010 by the American College of Cardiology Foundation

From the *Thoraxcenter, Erasmus University Medical Center, Rotterdam, the Netherlands; †Catharina Ziekenhuis, Eindhoven, the Netherlands; ‡Skejby Sygehus, Aarhus, Denmark; §Division of Cardiology, Swiss Cardiovascular Center, Bern, Switzerland; ‖The Cardiovascular Research Centre, St. Vincents Hospital, Fitzroy, Australia; ¶Cardiology Department, Christchurch Hospital, Christchurch, New Zealand; and the #Auckland City Hospital, Auckland, New Zealand. The authors have reported that they have no relationships to disclose. Drs. Okamura and Serruys contributed equally to the writing of this manuscript.

Manuscript received February 9, 2010; revised manuscript received April 20, 2010, accepted May 9, 2010.

The ABSORB Cohort A (Bioabsorbable Vascular Solutions First in Man Clinical Investigation: A Clinical Evaluation of the Bioabsorbable Vascular Solutions Everolimus Eluting Coronary Stent System in the Treatment of Patients With Single de Novo Native Coronary Artery Lesions) clinical trial was an open-label prospective multicenter study that demonstrated the feasibility of implanting revision 1.0 of the everolimus-eluting bioresorbable vascular scaffold (Abbott Vascular, Santa Clara, California) and showed a low rate of major adverse cardiac events at 2-year follow-up (1,2). Furthermore, multimodality imaging confirmed that the struts were substantially resorbed within 2 years (2). The 6-month intravascular ultrasound evaluation showed that the scaffold area shrank by 11% (3). In order to retain mechanical integrity and reinforce radial strength, modifications in the scaffold design (in-phase zigzag hoops linked together by 3 longitudinal bridges) and enhancement in polymer processing have been incorporated into revision 1.1 of the bioresorbable vascular scaffold (BVS). It has been evaluated in the ABSORB Cohort B study (4,5). The outcome of side branch (SB) jailing at follow-up is one focus of investigation of the BVS device, because struts at the orifice of the side branch can be bioresorbed and/or form a neointimal bridge/membrane.

Optical coherence tomography (OCT) with its high resolution is useful to evaluate the struts in detail. However, our understanding of the 3-dimensional (3D) relationship of the struts with the orifice of the SB is limited with the use of standard 2-dimensional (2D) OCT images. New generation Fourier-domain OCT (FD-OCT) provides an intracoronary image with less motion artifacts than conventional time-domain (TD) OCT due to faster frame rate and pullback speed, which enable 3D reconstruction of coronary vessels (6,7), allowing a direct visualization of the jailing process in vivo. Late evaluation using the same technique will help us to understand the fate of struts in jailed SB.

The FD-OCT technology was used optionally to assess the dimension of the struts in 6 out of the 12 centers participating in the enrollment of the ABSORB Cohort B. The purpose of this study is to assess with 3D FD-OCT how the SB orifice is jailed by BVS (revision 1.1) struts and to propose a descriptive classification of this jailed orifice.

Methods

Study design. The ABSORB Cohort B trial is a multicenter single-arm trial assessing the safety and performance of the BVS in the treatment of patients with a maximum of 2 de novo native coronary artery lesions. The recruitment started in March 2009 and was completed in November 2009. In this study, patients over the age of 18 years who had either stable or unstable angina pectoris or silent ischemia were suitable for inclusion. All treated lesions were de novo lesions in a native coronary artery with a maximum diameter of 3.0 mm, and a length of ≥14 mm for the 18-mm device, with a percentage diameter stenosis ≥50% and <100%, and a Thrombolysis In Myocardial Infarction flow grade of ≥1.

Major exclusion criteria were an acute myocardial infarction, unstable arrhythmias at presentation or left ventricular ejection fraction <30%, restenotic lesions, lesions located in the left main coronary artery, lesions involving an epicardial SB >2 mm in diameter by visual assessment, and the presence of thrombus or another clinically significant stenosis in the target vessel.

The study was approved by the ethics committee at each participating institution and each patient gave written informed consent before inclusion. The current analysis is a substudy of ABSORB Cohort B. Figure 1 shows the flow chart of the patients selected for this OCT substudy.

Study device. The revision 1.1 BVS is balloon expandable and consists of a polymer scaffold of poly-*L*-lactic acid coated with a thin layer of a 1:1 mixture of an amorphous matrix of poly-*D,L* (racemic)-lactic acid polymer, and 100 $\mu g/cm^2$ of the antiproliferative drug everolimus. The implant is radiolucent, but has 2 platinum markers at each end that allows for easy visualization on angiography and other imaging modalities. Everolimus suppresses neointimal hyperplasia by blocking growth factor–derived cell proliferation to arrest the cell cycle in the G1-S phase. The poly-*D,L* (racemic)-lactic acid allows controlled release of the everolimus such that 80% is eluted by 30 days; the elution rate, tissue concentration, and the dose density of everolimus are similar to that of the XIENCE V everolimus-eluting stent (Abbott Laboratories, Abbott Park, Illinois). Both poly-*L*-lactic acid and poly-*D,L* (racemic)-lactic acid are fully resorbable. The polymer degrades via a bulk erosion process through hydrolysis of the ester bonds in the backbone. The resulting lactic acid oligomers eventually leave the polymer matrix and are metabolized in surrounding tissues and blood by entering the pyruvate and Krebs energy cycles. The time for complete absorption of the polymer backbone is predicted from pre-clinical studies to be about 2 years, whereas the polymer coating is absorbed in a faster time frame.

Abbreviations and Acronyms

2D = 2-dimensional
3D = 3-dimensional
BVS = bioresorbable vascular scaffold
FD = Fourier domain
OCT = optical coherence tomography
SB = side branch(es)
TD = time domain

Physically, the scaffold has struts with a thickness of 160 μm, a crossing profile of 1.4 mm, and consists of in-phase zigzag hoops linked together by 3 longitudinal bridges (Fig. 2A). These design changes allow a more uniform strut distribution, which provides greater/more uniform vessel wall support and drug transfer than the previous revision 1.0 BVS. Implant security has increased, such that dislodgement is unlikely, and the device can be stored at room temperature.

JACC: CARDIOVASCULAR INTERVENTIONS, VOL. 3, NO. 8, 2010
AUGUST 2010:836–44

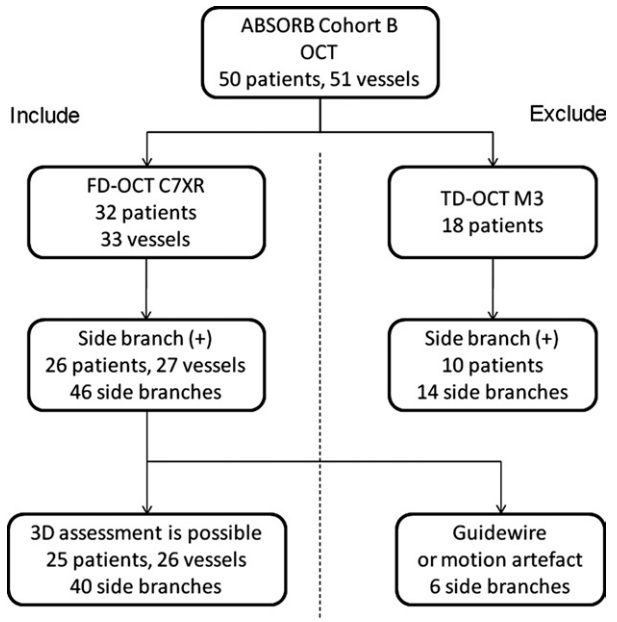

Figure 1. Flow Chart of Patient Selection

Flow chart shows the patient selection for ABSORB Cohort B (A Clinical Evaluation of the Bioabsorbable Everolimus Eluting Coronary Stent System in the Treatment of Patients With de Novo Native Coronary Artery Lesions). FD = Fourier domain; OCT = optical coherence tomography; TD = time domain; 3D = 3-dimensional.

OCT system. Intravascular imaging using either TD-OCT (M3 system, LightLab Imaging Inc., Westford, Massachusetts) or FD-OCT (C7-XR system, LightLab Imaging) was optionally performed after the procedure. Due to slower pullback, 3D reconstructions of TD-OCT were of poor quality, and these analyses are not included in our report. We used a FD-OCT system with a scanning laser as a light source, which is swept over a range of wavelengths between 1,250 and 1,350 nm (8). In order to create the OCT images, the echo-time delay and the amplitude of light reflected from the tissue microstructure at different depths are determined by processing the interference between the tissue sample and a fixed reference mirror. The imaging depth is approximately 1.5 mm into tissue with an axial resolution of 15 to 20 μm and a lateral resolution of 25 to 30 μm. The 2.7-F OCT imaging catheter (Dragonfly, LightLab Imaging) has a short monorail design and contains the fiber optic core that rotates within a translucent sheath. The imaging catheter is connected at its proximal end to the imaging console that permits real-time data processing and the 2D representation of the backscattered light in a cross-sectional plane.

Procedure. The 3.0 × 18 mm revision 1.1 BVS was implanted after mandatory pre-dilation. Because ostial lesions >40% involving an epicardial SB >2 mm in diameter were excluded, there was no attempt to wire the SB present in the treated segment. The OCT imaging catheter was advanced distal to the BVS over a 0.014-inch conventional

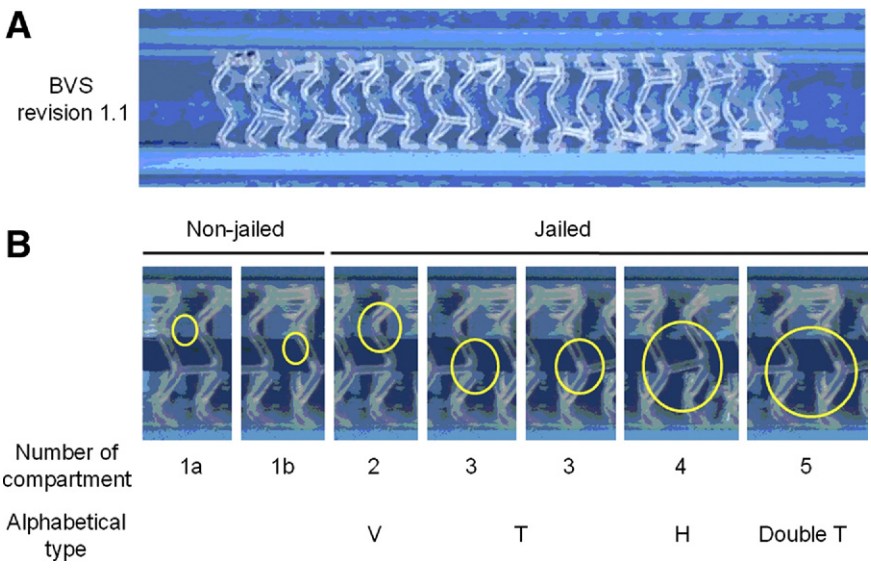

Figure 2. The Revision 1.1 BVS Designs and Classification of Jailed SB

(A) The bioresorbable vascular scaffold (BVS) has polymeric struts with a thickness of 160 μm and consists of in-phase zigzag hoops linked together by 3 longitudinal bridges. **(B) Yellow circles** represent the orifice of the side branch (SB). A nonjailed SB is defined as the complete absence of struts across the orifice (1a) or BVS struts located over the orifice without compartmentalization (1b). Jailed SB orifices are separated into various compartments. Types of SB jailing are expressed in alphabetical letters given according to resemblance of the strut structure across the orifice.

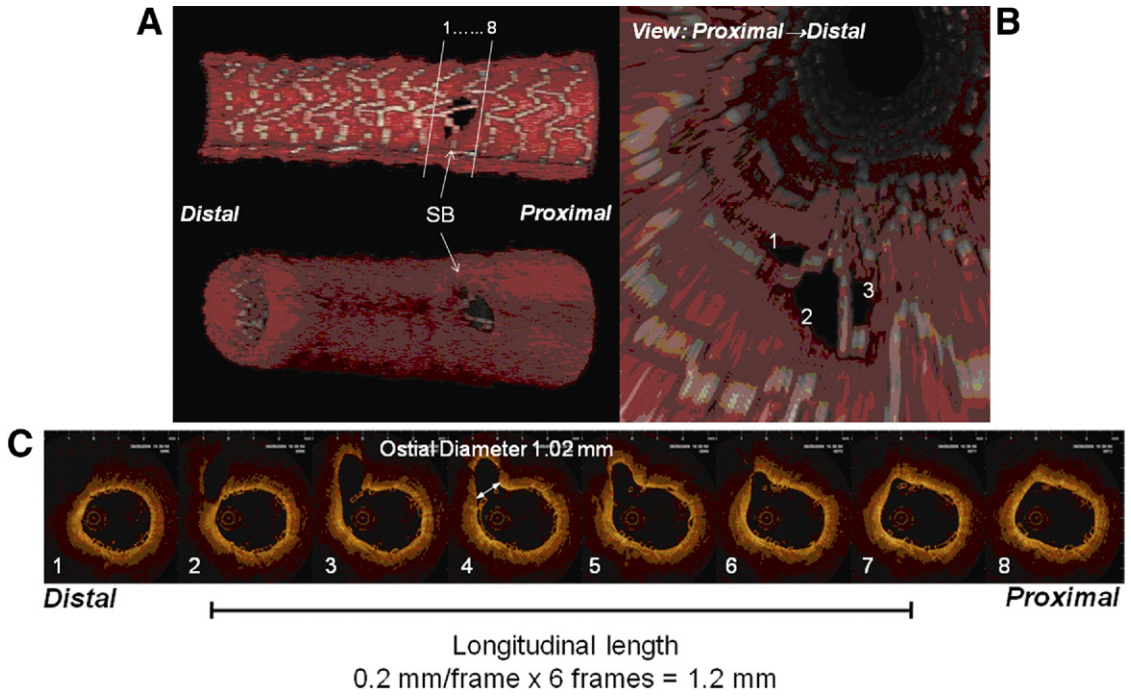

Figure 3. Representative Case of 2D and 3D Assessment for Jailed SB

(A) Three-dimensional volume rendered images and **(B)** virtual endoscopic view from the proximal site of the jailed SB. Three compartments are clearly seen. **(C)** Consecutive frames of optical coherence tomography images from immediately distal to immediately proximal to the SB. Longitudinal length was calculated using number of frames containing a SB. The maximal ostial diameter was measured on optical coherence tomography cross sections. 2D = 2-dimensional; other abbreviations as in Figures 1 and 2.

angioplasty guidewire. The pullbacks were performed during a continuous injection of 3 to 4 ml/s of X-ray contrast (Iodixanol 320, Visipaque, GE Healthcare, Cork, Ireland) injected at a maximum pressure of 300 psi through the guiding catheter using an injection pump (Mark-V ProVis, Medrad Inc., Indianola, Pennsylvania) after the intracoronary administration of 0.2 mg nitroglycerin. Images were acquired at 100 frames/s and an automated pullback speed of 20 mm/s. All patients received aspirin (>75 mg) daily for life and clopidogrel 75 mg daily for a minimum of 6 months.

OCT analysis. The pullback images were reviewed on the LightLab Imaging OCT proprietary offline workstation. The images were calibrated based on the reflection of the imaging catheter, which is the standard calibration technique for this system.

A 2D assessment of SB jailed by BVS struts was made by measuring the maximum diameter (D) of the SB orifice in the OCT cross section that shows the maximum opening of the orifice. The longitudinal length (L) was calculated as follows: 1) The first OCT cross section in which the SB was noted was bookmarked; 2) the number of consecutive OCT cross sections showing the orifice of the SB was counted; and 3) the length was then calculated by multiplying the number of consecutive cross sections by the frame thickness (0.2 mm/frame) (Fig. 3). Because the shape of SB orifices can be closely related to an oval (ellipse), an approximate area of SB orifice was calculated as follows:

$$\text{Orifice area} = 1/4 \times \pi \times D \times L$$

In order to make the 3D reconstruction, bitmap (704 × 704 pixels) sequences of the OCT image files were generated. Every single strut was detected in each OCT cross section. The 3D images were reconstructed using volume-rendering software (INTAGE Realia, KGT, Tokyo, Japan). Image calibration was performed with transverse resolution (scan diameter divided by pixel size) and longitudinal resolution (pullback speed divided by frame rate, usually 0.2 mm). The ostia of the SB were assessed visually and the number of strut-free compartments was categorized as follows. *Non-jailed side branch:* Either, no strut over the SB orifice is present or 1 of the BVS struts is present over the SB orifice but does not compartmentalize the orifice. *Jailed side branch:* The BVS struts separate the SB orifice into n compartments. The distribution of the struts creates different patterns of compartments: Subtypes V, T, H, and double T (Fig. 2B).

Statistics. Discrete variables are presented as counts and percentages. Continuous variables are presented as mean ±

JACC: CARDIOVASCULAR INTERVENTIONS, VOL. 3, NO. 8, 2010
AUGUST 2010:836–44

Table 1. OCT Quantitative Analysis (2D and 3D) (n = 40)

Lumen area at SB, mm^2	7.68 ± 1.34
Scaffold area at SB, mm^2	7.66 ± 1.16
Transverse orifice diameter, mm	1.2 ± 0.5
Longitudinal orifice diameter, mm	1.2 ± 0.5
Area of side branch orifice, mm^2	1.16 ± 1.02
Number of compartments	2.0 ± 1.1 (2, 1–3)

Values are mean ± SD (median, interquartile range).
OCT = optical coherence tomography; SB = side branch; 2D = 2-dimensional; 3D = 3-dimensional.

SD and ranges. Statistical analyses were performed with use of SPSS version 16.0 (SPSS Inc., Chicago, Illinois).

Results

A total of 101 patients were enrolled in the ABSORB Cohort B study. Fifty-one OCT pullbacks (51 scaffolds) at baseline were analyzed by the core lab (Cardialysis B.V., Rotterdam, the Netherlands). Eighteen scaffolds were imaged with TD-OCT (M3 system), and 33 scaffolds were imaged with FD-OCT (C7-XR system). Of these 33 FD-OCT imaged lesions, 27 treated segments had 46 SB covered by the scaffold struts. Six side-branch ostia were obscured by guidewires (n = 4) or had significant motion artifacts (n = 2) and were eventually excluded from this study. Thus, 40 SB ostia were analyzable in 25 patients (1 patient had 2 scaffolds). Patients were mostly men (72%) and had an age range from 40 to 79 years. The left anterior descending artery was the most frequently imaged artery (73.1% of cases).

The results from the 2D OCT analysis are presented in Table 1. Lumen area and scaffold area of the treated vessel at the site of the studied SB were 7.68 ± 1.34 mm^2 and 7.66 ± 1.16 mm^2, respectively. All but 2 scaffolds were well apposed at the site of the SB. The maximum diameter of the SB orifice and the longitudinal length of the SB were similar, both measuring 1.2 ± 0.5 mm. The calculated area of the studied side-branch orifice generated by these parameters was 1.16 ± 1.02 mm^2.

In 3D OCT analysis, the jailed SB orifice was subdivided into 2.0 ± 1.1 (range 1 to 4) compartments by the BVS struts. A total of 16 SB were nonjailed. The remaining 24 orifices showed different degrees and patterns of compartmentalization (Table 2).

Table 2. Frequency of Type

Type (No. of Compartments)	% (No. of Observations)
Nonjailed (1)	40% (16)
Jailed	
V (2)	25% (10)
T (3)	25% (10)
H (4)	10% (4)
Double T (5)	0
Total	100% (40)

A representative case is shown in Figure 3. In 2D cross-sectional OCT analysis, the area of SB orifice was measured as 0.96 mm^2. The 3D OCT images demonstrate clearly that the SB orifice is jailed and separated into 3 compartments (Type T). The other representative 3D images of SB compartmentalization Types V, T, and H are illustrated in Figure 4. Types V, T, and H clearly separate the jailed SB orifice into 2, 3, and 4 compartments, respectively.

Figure 5 shows the impact of the SB orifice area on the number of compartments delineated by the overhanging struts. Below 2.0 mm^2, the number of compartments can vary between 1 and 4. Beyond 2.0 mm^2, the number of compartments observed is 3 or 4. By protocol, no SB with

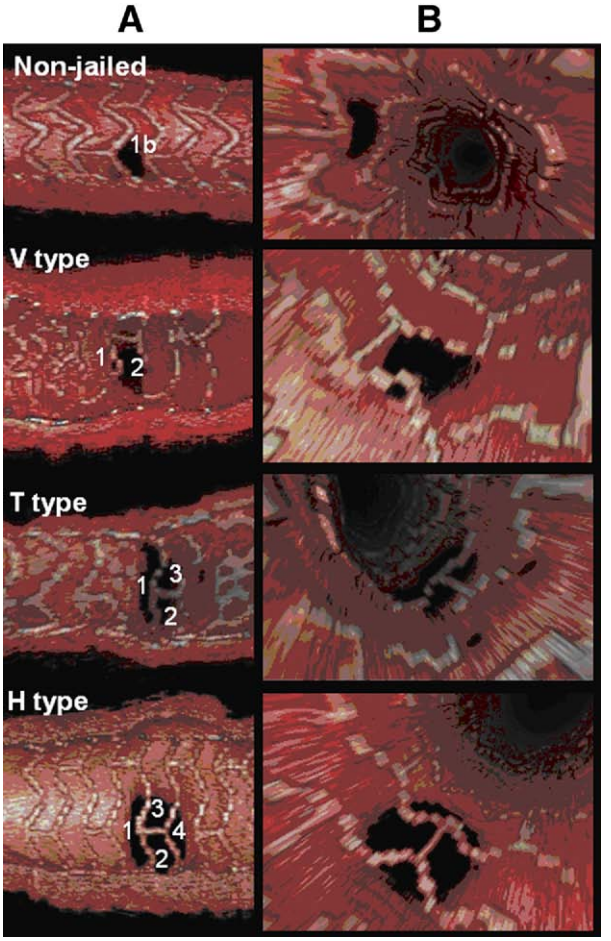

Figure 4. Three-Dimensional Assessment of Nonjailed and Types V, T, and H Jailed SB

Three-dimensional assessment of nonjailed and Types V, T, and H jailed SB: volume rendering **(A)**, virtual endoscopy **(B)**. Abbreviation as in Figure 2.

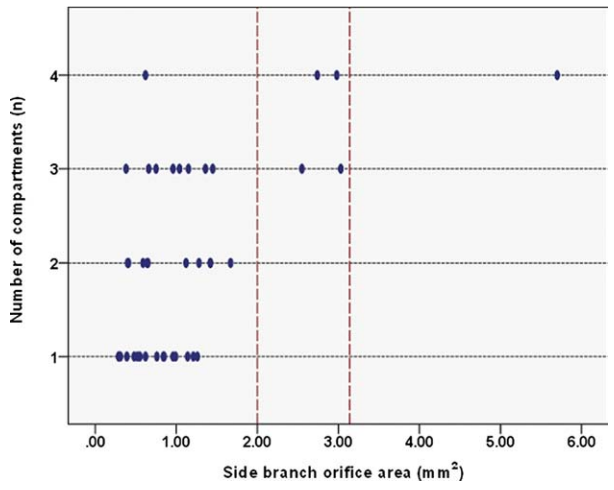

Figure 5. Impact of the SB Orifice Area on the Number of Compartments Delineated by the Overhanging Struts

A SB orifice with an area of 3.14 mm^2 corresponding to an ostium of 2 mm, which is the largest SB diameter acceptable according to the study protocol. Abbreviation as in Figure 2.

a diameter >2 mm (and orifice area ≥3.14 mm^2) should have been included. Inclusion of 1 case with a SB orifice area of 5.7 mm^2 could be considered as a protocol violation, but it concerns a large septal branch and not an epicardial SB.

Discussion

In the OCT substudy of the ABSORB Cohort B treated with BVS revision 1.1, 3D reconstruction with C7-XR FD-OCT system was feasible in 87% (40 of 46) of SB. The 3D reconstructed images enabled detailed assessment of both the longitudinal and cross-sectional relationship between the jailed SB orifice and the overhanging BVS struts. Furthermore, the pattern of the jailed orifice can be easily classified in vivo according to: 1) the structural configuration of the overhanging struts (Types V, T, H, double T); and/or 2) the number of compartments delineated by the struts.

This is the first report of the combination of 2D and 3D OCT assessment evaluating the relationship between the polymeric struts of the BVS and the orifice of coronary side branches. Such an assessment has never been routinely performed for metal stents although the first report of 3D OCT imaging of 3 arteries implanted with metallic stents dates back to November 2008 (7). Unlike metal stent struts, the polymeric struts of the BVS are completely translucent to OCT (with only endoluminal and abluminal surfaces backscattering) without shadowing behind them (2). The combination of these characteristics provides a unique

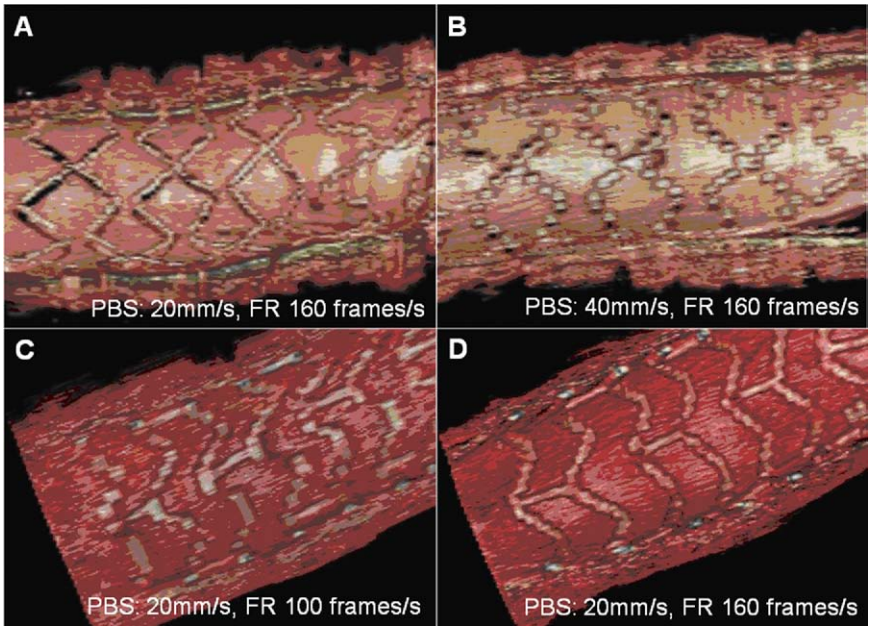

Figure 6. Impact of Pullback Speed and Frame Rate on 3D Image

(A,B) Three-dimensional (3D) images in the same treated segment obtained at a different pullback speed (PBS) but the same frame rate (FR). **(C,D)** 3D images in the same treated segment of a patient treated with bioresorbable vascular scaffold obtained with 2 different optical coherence tomography systems. **(C)** C7-XR system (PBS: 20 mm/s, FR: 100 frames/s); **(A,B,D)** Terumo optical frequency domain imaging system (PBS: 20 or 40 mm/s, FR: 160 frames/s). Abbreviation as in Figure 1.

JACC: CARDIOVASCULAR INTERVENTIONS, VOL. 3, NO. 8, 2010
AUGUST 2010:836–44

opportunity for OCT to assess the interaction between polymeric struts and side branches.

This study demonstrates the feasibility of a 3D reconstruction of the coronary artery treated with a polymeric scaffold using a new generation of commercially available FD-OCT system. Because FD-OCT has a higher frame rate (100 frames/s) than conventional TD-OCT system (20 frames/s), FD-OCT allows faster pullback speed (20 mm/s) than TD-OCT (3.0 mm/s). Due to the fast pullback speed, the scanning time of the treated segment (18 mm) is less than 1 s, considerably reducing the motion artifacts caused by the beating heart. In addition, a large scanning diameter (9.6 mm) enables visualization of the SB, whereas high signal-noise ratio results in good quality 3D images. However, in 4 of 6 SB, shadowing by the guidewire hindered visualization of the SB, making 3D assessment impossible. Because the FD-OCT system has a rapid exchange system utilizing a conventional guidewire, artifacts by such a metallic wire might be an inherent limitation of this technology, unless the guidewire is removed prior to the final pullback, an approach used by some investigators in this trial.

In the present study, the longitudinal spatial resolution (200 μm) is 10 times poorer than the cross-sectional resolution (approximately 20 μm) due to the speed of the pullbacks (20 mm/s) and the frame rate (100 frames/s). Consequently, the longitudinal length of the SB orifice might be overestimated and the calculated orifice area might be greater than its actual area. It is noteworthy that faster pullback may affect the resolution of 3D images and result in a grainy longitudinal reconstruction, whereas higher frame rates enhanced the 3D reconstruction. In one of our cases, we obtained OCT images of the same BVS implanted segment at different frame rates (100 frames/s [C7-XR system] vs. 160 frames/s [Terumo optical frequency domain imaging system, Terumo Corp., Tokyo, Japan]) but with the same pullback speed of 20 mm/s. These conditions of acquisition yield a longitudinal resolution of 200 and 125 μm, respectively. Figure 6 illustrates 3D images of both systems. The longitudinal resolution (frame thickness) depends on both the pullback speed and the frame rate. Pullback speed will increase or reduce motion artifact, whereas faster frame rates will enhance 3D reconstruction of OCT pullbacks.

In addition to the conventional 2D analysis (e.g., quantitative assessment of luminal dimension, semiqualitative assessment of changes in strut appearance) (2), FD-OCT imaging with 3D reconstruction could potentially provide us with long-term information on anatomical modification seen at the site of bifurcations treated with the fully

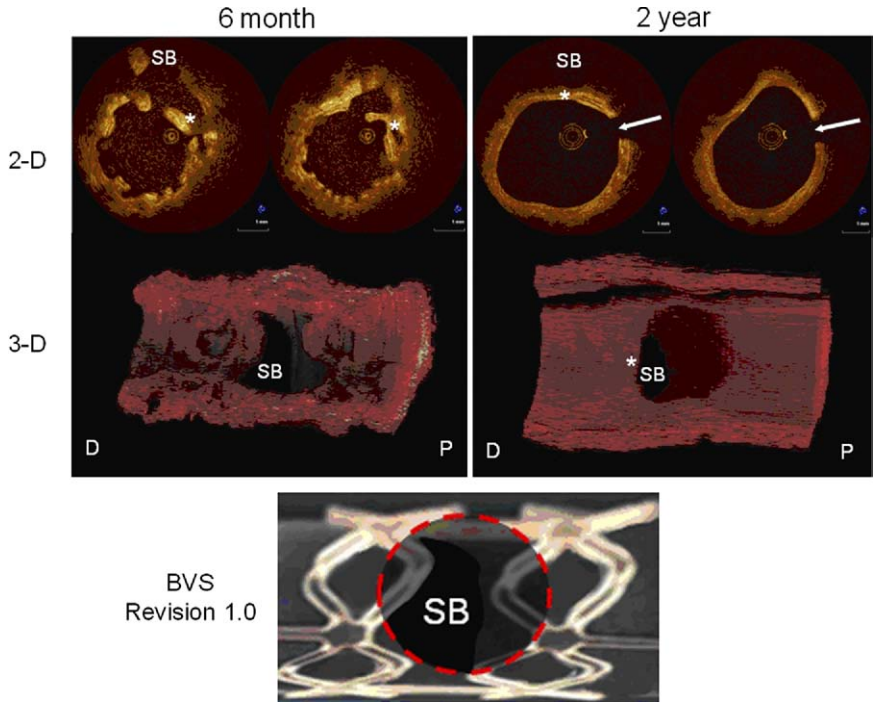

Figure 7. Serial 2D and 3D OCT in Cohort A

Struts in front of a SB were covered by neointimal tissue at 6 months. At 2 years, the neointimal tissue further extended to form a membranous structure bridging over the orifice (*, neointimal bridge). The **white arrows** indicate the shadowing effect of the guidewire. D = distal rim of the side branch orifice; P = proximal shoulder of the orifice; other abbreviations as in Figures 1 and 2.

bioresorbable vascular scaffolds. In the first-in-man trial (ABSORB Cohort A), which enrolled 7 patients with serial—post-procedure, 6-month, and 24-month—OCT follow-up, the neointimal tissue covering the struts located in front of a SB tended to form a membranous structure partially bridging the orifice at the distal side of its rim; this structure has been tentatively described as a "neointimal bridge" and appeared as a de novo semilunar extension of the pre-existing carina. An example of this structural modification is illustrated in Figure 7. Three-dimensional reconstruction of the OCT image was serially obtained at 6 months and 2 years. At 6 months, the overhanging struts partially jailing the SB were still identifiable but appeared thickened and covered by tissue. At 2 years, the struts structures covering the proximal side of the SB orifice have been fully incorporated into the vessel wall, whereas the struts located at the distal side of the orifice tended to form an extended new carina of a semilunar shape. Presumably, the creation of these neointimal bridges can be the result of a complex and dynamic interaction between the bioresorbable polymeric struts, the vessel wall and the vessel wall shear stress and these late alterations are rendered possible by the absence of permanent metallic caging of the vessel wall. As shown in Figure 3, it is challenging to mentally reconstruct from 2D cross-sectional images the 3D changes in configuration of the struts overhanging the orifice. Therefore, 3D reconstruction will be indispensable for early and late evaluation of a SB orifice crossed over by polymeric struts.

In the current analysis, we propose a classification of the jailing struts based on the number of compartments delineated by the struts as well as on their geometric configuration in front of the orifice. Although the compartmentalization of SB by BVS struts occurs at random, the likelihood to find complex-shaped compartments at the site of the SB increases with the diameter of its orifice. In order to exemplify this speculation, we performed a phantom experiment using the BVS. The BVS was deployed in the main branch of a silicon model overlapping a 2.5-mm SB creating a higher number of compartments (up to 7) than seen in our human clinical cases. In this model, the capability to overstretch struts overhanging SB orifices with a balloon was tested (Fig. 8). Acutely, the number of compartments could affect the flow distal into the SB and complex compartmentalization and strut configuration might affect the rewiring of the SB. The long-term fate of the struts across the SB orifice will be further investigated at follow-up in the Cohort B patients.

Overhanging struts in front of SB orifice have always been sources of concern as far as thrombosis, alteration of

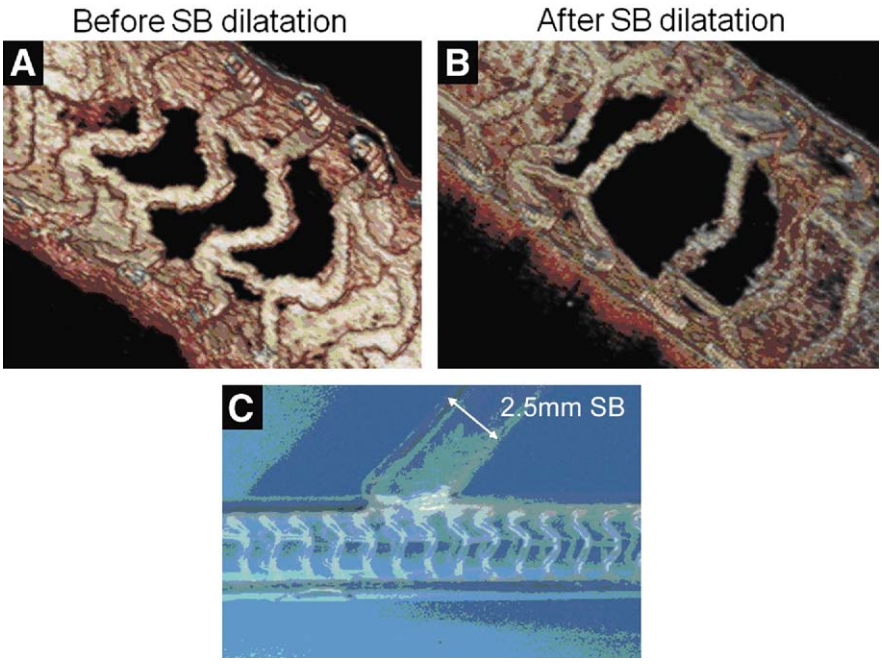

Figure 8. Impact of Dilation for SB Jailed by BVS Strut: Phantom Study

(A,B) Three-dimensional reconstruction of optical coherence tomography pullback. **(A)** Bioresorbable vascular scaffold was deployed in the main vessel crossing over a 2.5-mm SB orifice in silicon model. The SB was compartmentalized into 6 (Type V + double H). **(B)** After SB dilation, a configuration of jailed SB orifice by the bioresorbable vascular scaffold strut was modified. **(C)** Photo of the bioresorbable vascular scaffold in the silicon phantom model having the 2.5-mm SB. Abbreviations as in Figures 1 and 2.

shear stress, embolization, or endothelial coverage are concerned. In future trials performed with BVS, we will monitor and, if necessary, correlate the occurrence of event with the frequency and complexity (using the classification in semiquantitative fashion) of the jailed side branches using the proposed classification.

Study limitations. The study is limited by the small number of patients. Moreover, a correlation between the proposed classification and long-term outcomes is not assessed in the present study and awaits for medium- and long-term follow-up. The reproducibility of 3D OCT reconstruction has not yet been established. Current version of volume rendering software does not support quantitative 3D measurements; therefore, we calculated orifice area using 2D diameters.

Conclusions

3D reconstruction of the SB orifice was feasible with novel FD-OCT imaging. Using such images, the jailed SB orifice can be classified according to the number of compartments and the configuration of overhanging struts. The impact of this classification on the fate of these fully bioresorbable struts covering SB ostia will be further investigated at follow-up.

Acknowledgments

The authors thank Richard J. Rapoza, Krishna Sudhir, and Susan Veldhof (Abbott Vascular) for their expert review of this manuscript. The authors also thank Juan Luis Gutiérrez-Chico, MD, and Michael Magro, MD (Thoraxcenter), for their careful reading and critical review of the manuscript.

Reprint requests and correspondence: Dr. Patrick W. Serruys, Thoraxcenter, Bd583a, Dr. Molewaterplein 40, Rotterdam 3015-GD, the Netherlands. E-mail: p.w.j.c.serruys@erasmusmc.nl.

REFERENCES

1. Ormiston JA, Serruys PW, Regar E, et al. A bioabsorbable everolimus-eluting coronary stent system for patients with single de-novo coronary artery lesions (ABSORB): a prospective open-label trial. Lancet 2008; 371:899–907.
2. Serruys PW, Ormiston JA, Onuma Y, et al. A bioabsorbable everolimus-eluting coronary stent system (ABSORB): 2-year outcomes and results from multiple imaging methods. Lancet 2009;373:897–910.
3. Tanimoto S, Bruining N, van Domburg RT, et al. Late stent recoil of the bioabsorbable everolimus-eluting coronary stent and its relationship with plaque morphology. J Am Coll Cardiol 2008;52:1616–20.
4. Ormiston JA, Serruys PW. Bioabsorbable coronary stents. Circ Cardiovasc Interv 2009;2:255–60.
5. Okamura T, Garg S, Gutierrez-Chico JL, et al. In-vivo evaluation of stent strut distribution patterns in the bioabsorbable everolimus-eluting device: an OCT ad hoc analysis of the revision 1.0 and revision 1.1 stent design in the ABSORB clinical trial. EuroIntervention 2010;5:932–8.
6. Yun S, Tearney G, de Boer J, et al. High-speed optical frequency-domain imaging. Opt Express 2003;11:2953–63.
7. Tearney GJ, Waxman S, Shishkov M, et al. Three-dimensional coronary artery microscopy by intracoronary optical frequency domain imaging. J Am Coll Cardiol Img 2008;1:752–61.
8. Barlis P, Schmitt JM. Current and future developments in intracoronary optical coherence tomography imaging. EuroIntervention 2009; 4:529–33.

Key Words: bioresorbable vascular scaffold ■ optical coherence tomography ■ side branch ■ stent.